Bayesian structural reliability updating using a population track record

de Vries, R.; Steenbergen, R. D.J.M.; Vrouwenvelder, A. C.W.M.

DOI
10.1016/j.ress.2024.110644

Publication date
2024

Document Version
Final published version

Published in
Reliability Engineering and System Safety

Reliability Engineering and System Safety 255 (2025) 110644

Contents lists available at ScienceDirect

Reliability Engineering and System Safety

journal homepage: www.elsevier.com/locate/ress

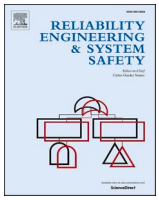

Bayesian structural reliability updating using a population track record

R. de Vries [a,b,*], R.D.J.M. Steenbergen [a,c], A.C.W.M. Vrouwenvelder [a,b]

[a] Reliable Structures, Netherlands Organization for Applied Scientific Research (TNO), Delft, the Netherlands
[b] Faculty of Civil Engineering and Geosciences, Delft University of Technology, Delft, the Netherlands
[c] Faculty of Engineering and Architecture, Ghent University (UGent), Ghent, Belgium

ARTICLE INFO

Keywords:
Structural reliability
Existing structures
Bayesian updating
Track record
Proven strength

ABSTRACT

In the assessment of existing structures, it is uncommon to consider a track record of the structural performance of the structure itself or similar structures. However, the structure's proven strength in service could play a significant role, along with the performance of similar structures in the population. Because the population track record does not apply in the design of new structures, it is not encountered in design standards. An assessment that does not incorporate the track record may conclude insufficient structural reliability whilst, in reality, the reliability is satisfactory. In the suggested approach, information obtained from laboratory experiments is combined with the track record in a Bayesian way to assess a structure's reliability. As a case study for this article, the reliability of the connection strength between wide slab floor elements is considered. Although laboratory tests indicate poor connection strength, the track record indicates just one failure and many well-performing floors. It is found that considering the time-dependent nature of structural reliability is vital for understanding how proven strength develops from the completion of the structure to its usage today. The number of similar objects in the population that show satisfactory performance is varied and is shown to have a significant effect when its number grows. The presented method and case study show that reliability assessments incorporating a track record enable more accurate structural reliability predictions for existing structures.

1. Introduction

In the design and evaluation of structural systems, structural reliability analysis consists of a collection of techniques and models that can be used for probability- and risk-based decision-making. Application may be found in codes and guidelines for structural engineering, sometimes explicit but in most cases in the form of so-called semi-probabilistic procedures. The main task in structural reliability analysis is the estimation of the lifetime (or annual) failure probability for a given structure. As input, the calculation procedure requires structural behaviour models as well as a probabilistic description of all relevant actions, material properties and geometrical parameters. In fact, the establishment of these models themselves is already an essential part of the structural reliability analysis. Here, the current article proposes a next step by including track record information in the behaviour models used for the structural reliability analysis. The application of the proposed reliability updating method will be illustrated by a practical example.

On 27 May 2017, part of a parking garage being built at Eindhoven Airport in the Netherlands collapsed [1]. The building was almost finished and would be put into use a month later. Wide slab floors were used in the construction of the building. In this floor system, thin prefabricated concrete slabs are placed first, followed by additional reinforcement and an in-situ concrete layer. As a result of the collapse, further research into the resistance of wide slab floors was initiated. In particular, the mechanical properties of the longitudinal joint between wide slabs to form a continuous span were studied in a laboratory setting, resulting in new information about the mean capacity and the coefficient of variation for various failure mechanisms [2]. In addition, it is known that similar floor slabs were used in thousands of buildings, all performing without noticeable shortcomings under the applied load conditions over the past decades. So, besides the information from the laboratory experiments, there is the knowledge of a single failure but also many well-performing floors in an in-situ environment; the latter is called the track record.

Therefore, as input to the structural reliability calculation, two types of information need to be taken into account: a) the information from the laboratory experiments and b) the information from the track record. Including a) is established knowledge, e.g. see Annex D of [3]; however, a conceptual reliability framework to include b) is not evident

* Corresponding author.
E-mail address: rein.devries@tno.nl (R. de Vries).

https://doi.org/10.1016/j.ress.2024.110644
Received 13 September 2023; Received in revised form 18 October 2024; Accepted 12 November 2024
Available online 20 November 2024

and is therefore the subject of the current article. Note that to some extent, we may conceive the uncertainties under a) as being part of the model uncertainty θ and the uncertainties belonging to b) as part of the conversion factor η as introduced in EN 1990 [3] and ISO 2394 [4]. In Section 2, the track record to be included in the reliability analysis is described. It describes the type of information and how it relates to the limit state function. In Section 3 it is explained how the track record is accounted for in a reliability analysis using Bayesian updating and the Monte Carlo method. Sections 4 and 5 describe an application and the results of the proposed method in the context of wide slab floors. Sections 6 and 7 conclude the article with a discussion and conclusions.

2. Track record for reliability analysis

2.1. State of information

To assess the reliability of a structural system, all relevant information should be taken into consideration. In this respect, one should firstly think of information related to the physical properties of the structure (dimensions, material properties) and actions, including the available information about the corresponding statistical models. It will be clear that for the assessment of an existing structure next to prior information also results of individual inspections and other observations may or should also be considered. In addition, where possible, one may include observations made on other similar structures. This is what is called the 'track record' in this article.

If more information about which parameters are important or more detailed information about these parameters is gathered, the reliability measure will likely change. In this light, even bad news can lead to an increase in reliability [5].

2.2. Structural reliability

The failure probability of a given structure may be formulated as:

$$P_f = P(Z < 0) \tag{1}$$

where $Z = g(\mathbf{X})$ indicates the limit state function of the failure mechanism or the combination of failure mechanisms under consideration. In this formulation, $\mathbf{X}$ is a vector containing the random variables. A typical limit state function is given as $Z = g(R, G, Q) = R - (G + Q)$, with R the resistance, G the permanent action and Q the variable action. The resistance R is traditionally written as model uncertainty (θ_R) times the resistance following from theoretical models or laboratory experiments (Annex D of [3]). However, here the information from the track record is missing; this is discussed in the following paragraphs.

2.3. Track record

In the assessment of existing structures, the in-situ performance of the structure under investigation or of similar structures in a population is known. In the track record information that some structures in the population have failed in the past while others are performing well until the moment of assessment is included. The observations of the type 'the resistance is larger than a not exactly specified load' for a known population is referred to as the 'mega-experiment'. It is essential to include the mega-experiment since in an actual building the structural performance of a structural element could be different from the performance in laboratory circumstances. Examples are:

- the deviating behaviour of a floor in-situ compared to laboratory tests (including scale effects and system effects such as spreading of load effects);
- increasing the internal lever arm in a floor structure due to the structural contribution of a finishing layer that is not included as such in the design calculation;
- membrane or arch effects;
- redistribution of section forces.

The information resulting from the mega-experiment takes place on the level of complete structures instead of on the level of details, girders, columns, slabs, etc.

When including information from a track record, the choice of the (sub)population is of significant importance. For example, it does not make sense to judge the reliability of a certain structure with a known weak detail pointing at the large group of well-functioning structures where this detail is not present. Such information is important and must be carefully included insofar as this is possible on the basis of knowledge of different types of details, embodiments, etc. Where relevant, subpopulations therefore need to be distinguished and assessed.

2.4. Structural reliability including the track record

The reliability of existing structures should be assessed using all information available at the time of the assessment. The updated probability of failure, on basis of a calculation model and given the available data is expressed as:

$$P_f = P(Z < 0 \mid D) \tag{2}$$

where Z indicates the limit state function of the object under consideration as before and D the relevant data. Eq. (2) is different from Eq. (1), because of the presence of D behind the condition sign. The notation D is used for the data – as they are not typically observations of random variables in the limit state function. The data encompasses the real-world performance of an object or of a set of similar objects, i.e. the track record. The object, thought to be part of a population, may be a structure, a structural component, and so on. Its track record, as stated, contains two sources of information:

1. Performance of the object itself, up to the time of assessment. This information will normally be positive, i.e. no failure in the past years. If the structure had failed there would be no point in (future) reliability predictions. Of course, inspections or "near escapes" may lead to a lower reliability estimate compared to the initial estimate, but that is not a part of the present article.
2. Performance of similar objects, including the (loading) conditions. Known failures and non-failures should be included. Similarity (mathematically expressed by the degree of correlation) is closely related to the definition of the population discussed next.

Including the two sources of information as stated above, the data may be expanded as:

$$D = [S^{(t)}, F_1, F_2, \ldots, S_1, S_2, \ldots] \tag{3}$$

where $S^{(t)}$ indicates survival of the object itself up to the time of assessment, $F_i = \{Z_i < 0\}$ indicate the failures of similar objects and $S_j = \{Z_j \geq 0\}$ indicate the similar objects that have survived.

3. Reliability updating using a track record

3.1. General principle

In the process of reliability updating use is made of statistical inference via the application of the Bayesian method, as already introduced in 1939 in the first edition of the book *Theory of Probability* by Jeffreys [6]. It is the most referenced work that describes the basis of the Bayesian method as it is used today [7]. The method gained more attention later, largely thanks to the work of Lindley [8], Box and Tiao [9] and others. At its core is Bayes' theorem, which may be expressed as (other formulations exist as well):

$$\mathrm{P}(H|D) = \frac{\mathrm{P}(D|H)\mathrm{P}(H)}{\mathrm{P}(D)} \tag{4}$$

where H refers to a hypothesis (e.g. the value of model parameters) and D to the observations or data. Benjamin and Cornell [10] describe the Bayesian updating of engineering models and the decision-making process within a civil engineering context. Others followed with the application of Bayesian updating for mechanical, computational, system identification and structural health monitoring applications [11–15]. Of particular interest in the context of this study is the updating of structural reliability associated with existing structures. Especially in the adoption of new structural systems where experience is missing, design and execution flaws are more likely to occur. Bayesian methods provide a way to assess the performance of engineering models and update the associated uncertainty [16].

3.2. Prior distribution and likelihood

In Bayesian statistics, the prior distributions of the parameters that need to be updated allow for the insertion of subjective knowledge. Past experience and a degree of uncertainty may both be incorporated in the selection of prior distributions and their parameters. In cases where less subjectivity is desired, noninformative priors (often in the form of uniform distributions) are used [6]. In the updating process, informative prior distributions are preferred, as noninformative prior distributions can lead to irrational outcomes [17]. By adopting low informative priors, only very little information is added based on common physical sense [18].

When Bayesian updating is performed based on a track record, the likelihood function evaluates the probability of observing the track record (D), given a hypothetical set of parameter values (H):

$$\mathrm{P}(D|H) = P\left(D_{\mathrm{c}|H} = D\right) \tag{5}$$

where $D_{\mathrm{c}|H}$ describes all possible outcomes of the calculated track record given H. In the current application, the track record concerns the survival or failure of the considered objects, but it may describe any performance-related property. For this reason, the generic formulation in Eq. (5) is used.

3.3. Calculation method

Several calculation methods can be applied to obtain the posterior distribution, $\mathrm{P}(H \mid D)$. In most cases, the explicit calculation of the marginal likelihood, $\mathrm{P}(D)$, is not required because it acts as a normalising constant [6]. Analytical calculations are possible when the prior and posterior distributions are from the same distribution family. It is then called a conjugate prior to the likelihood function [19]. The common (textbook) example involves a Bernoulli trial with a beta distribution for both the prior and posterior modelling successes and failures. However, in more complex engineering applications the computation of the posterior requires numerical calculation.

When the number of possible outcomes is finite and small, numerical integration may be used to calculate the posterior directly using the (nested) summation of the probabilities. If continuous random variables are used, discretisation of their distribution functions is necessary. Finely discretised distributions combined with a large number of random variables often lead to an intractable problem – especially when the calculation of the likelihood is computationally expensive. In these circumstances, Monte Carlo simulation provides a solution. It should be realised that in this application the data is of the type $\{Z < 0\}$ or $\{Z > 0\}$ (see Section 2.4); in case of observations with the equality sign, a discretisation of the output space is necessary. In the application of Bayesian inference, two methods are generally distinguished in literature:

1. **Bayesian Monte Carlo (BMC)**: In the BMC method, the prior distributions are sampled n times. For each sample, the simulation is carried out to determine if the particular set of parameter values (H) gives rise to the desired behavioural outcome (likelihood evaluation). After the simulation, m parameter sets are stored which led to the observed data represented by the set D, and $n - m$ parameters sets that did not. Together, the m samples that led to the desired behaviour describe the posterior distribution [20,21].
2. **Markov Chain Monte Carlo (MCMC)**: In the MCMC method, a Markov chain is constructed which can subsequently be used to obtain samples from the posterior distribution. The Metropolis-Hastings [22,23] and Gibbs sampling algorithm [24] may be used to produce such a sequence. The construction of the chain is a gradual process, slowly converging to the desired distribution. For this reason, a so-called burn-in period is required.

In the current work, the BMC method is adopted, mainly because of its simplicity. Concerns have been raised about the efficiency of the BMC method and the possibility of incorrect results due to insufficient samples in the important regions [25]. However, these limitations are of general concern with the application of Monte Carlo methods. These issues are recognised, and more advanced strategies, such as importance sampling [26] and recursive stratified sampling [27], may be adopted to increase its efficiency. In the current research, efficiency has not been a limiting factor because the reliability indices are relatively low and the calculation procedure was written in C++, a programming language developed with performance in mind [28].

The proposed algorithm for a typical track record calculation using the BMC method is described in Appendix A. Because of the Monte Carlo implementation, the likelihood function may be implemented as an indicator function: given a particular realisation of the model parameters, it may be determined whether the track record matches the calculated track record or not – see Eq. (5). The likelihood function is thus not explicitly required to provide a measure of the likelihood, which would be difficult to compute given the numerous reliability calculations (including correlations and time-dependence) needed for its evaluation.

3.4. Reliability updating for a given model

The structural reliability updating is performed on the basis of a probabilistic calculation model $g(\mathbf{X})$ and a data set of observations D. The choice of both the calculation model g and the total population offering the data D is, to some extent, arbitrary. For example, one can choose a simple model in the limit state function of Eq. (2) and thus accept a large (model) uncertainty or a more accurate model with a larger modelling effort and less uncertainty. A large amount of uncertainty normally remains in the case of a large uninformative population, as possible differences in subpopulations are not accounted for. In the Bayesian reliability updating process, adding data contained in the track record to a simple model with large uncertainty will typically have a substantial effect. When the data is added to an accurate model with small uncertainty, the results will not change significantly. If the scope (population) was chosen to be very large, the data will contain greatly varying outcomes and the uncertainty in the posterior remains. Note that the level of reliability is also of influence.

In most cases, the uncertainty stems from a poor understanding of the structural resistance and possibly a part due to construction (human) error. Experiments in the laboratory are commonly employed to calibrate mechanical models such that they describe the resistance with greater accuracy. In the same way, the track record may be regarded as a real-world mega experiment. The same basic principles for updating on the basis of data experiments hold for both cases. The model uncertainty of the resistance (θ_R) functions as a generic 'basket' in which all uncertainty not explicitly accounted for is captured in a versatile manner by treating its mean and coefficient of variation as random variables within a Bayesian updating framework [29]. A helpful general form of

the limit state function where the resistance and load effect are incorporated is:

$$Z = g(\mathbf{X}) = \theta_R R - \theta_E(G + Q + \ldots) \quad (6)$$

where R is the resistance, θ_E the model uncertainty of the load effect, G the permanent load, Q the variable load, and so on. Another random variable, in particular another model uncertainty (e.g. θ_E), could also be used as a variable to be updated. But, this approach would be further from reality since it is believed that in this case there is primarily a lack of proper modelling with regard to the resistance. Also for that reason the updating process is performed per (sub)population in order to arrive at a representative model uncertainty.

3.5. Correlation modelling for the track record

The impact of the information following from the track record of the structure under consideration and from other structures depends largely on the degree of correlation between the random variables in the various limit states. Table 1 gives an overview of the most important correlations related to the stochastic parameters in Eq. (6). It is assumed the reference period for the variable load is chosen such that its subsequent realisations are independent. In most cases, the correlation between elements located in different buildings will be too small to have a significant effect; hence the correlation coefficient is 0. An autocorrelation coefficient of 1 for the resistance R implies a constant value over time, irrespective of possible deterioration trends. If the deterioration is implemented as a random process, the coefficient may be smaller than 1.

As mentioned before, special attention is required for the model uncertainty of the resistance θ_R. This model uncertainty takes into account the difference between the mathematical (or mechanical and material) model and the reality. This model uncertainty is regarded as a source of uncertainty, the size of which can be reduced by collecting more (structural element specific) information. In structural reliability calculations including the track record, the mean and the coefficient of variation of θ_R should be taken as stochastic parameters. They are believed to be different for each subpopulation because of the differences in the joint type and configuration. In addition, there is of course the variation between members in one subpopulation because of the different methods of execution, etc. Thus, the realisations of θ_R are independent for each individual structural element, but the mean value and coefficient of variation are fully dependent between elements since the elements belong to one subpopulation (empirical Bayes method).

To account for the correlation in time (autocorrelation) for the same element a time-dependent reliability analysis is performed within the BMC method. When viewed as Bayesian updating, the likelihood function is evaluated in each period to give the posterior (block period of 5 years, see Table 3). The next block will use the posterior as its prior distribution and evaluate the likelihood again. Effectively, the distributions of all time-independent parameters are updated each time step in the simulation (see Appendix A).

Table 1
Overview of correlations in time and between structural elements.

Symbol	Definition	In time (the same structural element)	Between elements, same building	Between elements, different buildings
G	Permanent action	1	[a]	0
Q	Variable action	0	[a]	0
R	Resistance	1	[a]	0
θ_E	Model uncertainty load effect	1	[a]	0
θ_R	Model uncertainty resistance	1	[a]	0
$m_{\theta R}$	Mean of θ_R	1	1	1
$V_{\theta R}$	Coefficient of variation of θ_R	1	1	1

[a] An appropriate value based on measurements, literature or expert judgement.

4. Case study

4.1. Wide slab floor connections

The theory presented in the previous sections has been applied in the context of wide slab floor systems. Traditionally, wide slabs span from load-bearing wall to load-bearing wall. The bottom reinforcement, included in the wide slab, is present along the entire length of the floor. Lattice girders are incorporated to be able to lift the slabs during production and construction, and to give sufficient strength during the pouring of the in-situ layer (Fig. 2). In addition, the lattice girders allow the precast wide slab and the in-situ concrete to bond together.

In the direction perpendicular to the span, where the slabs lie next to each other, normally only minimal forces will develop. A minor gap between the precast floor slabs exists. If the loads are small, no extra reinforcement in the in-situ layer is considered to be necessary according to Dutch building requirements. When higher loads are expected, the application of reinforcement over the joint is prescribed [30,31]. This situation arises in complex floor geometries where a positive bending moment is expected near the joint (Fig. 1). Top reinforcement would be added as well in the in-situ concrete layer to account for the support moments.

The connection reinforcement is placed onto the prefabricated wide plates, perpendicular to the joint, before pouring the in-situ concrete layer (Fig. 2). The design requirements assume sufficient bond and shear strength, such that yielding of the reinforcement governs the capacity – like in regular concrete element design. However, experiments revealed a substantial reduction in bending capacity compared to the case in which yielding reinforcement governs [2].

4.2. Connection detailing and failure mechanisms

Dutch standards prescribe the maximum distance between the (centre of the) lattice girder truss and the joint, and the minimum length of the connection reinforcement [30,31]. In the Dutch execution practice until mid-2017, the maximum distance between the lattice girder and the joint was typically relatively large (400 mm and due to execution tolerances distances up to 450 mm). The length of the connection reinforcement was not always on par with this large distance between the lattice girder and the joint. Therefore the effective length, i.e. the length of the connection reinforcement minus the distance between the lattice girder and the joint, varied. Due to this not-well thought-out-joint design, various additional failure mechanisms (see Fig. 3) can result in a reduced capacity – compared to the yielding of the connection reinforcement (the desired failure mechanism). Three detail types typically occur in existing buildings with wide slab floors manufactured before the collapse of the parking garage of Eindhoven Airport in 2017 (Fig. 2):

I. The connection reinforcement is equal to, or extends more than, 100 mm behind the lattice girders. All four identified failure mechanisms are possible.
II. The connection reinforcement extends less than 100 mm behind the lattice girders. Failure mechanisms 1, 2 and 4 are possible.
III. The connection reinforcement ends before or at the location of the lattice girders. Only failure mechanisms 1 and 4 are possible.

On the basis of tests and mechanical schematisations, three failure mechanisms additional to the regular yielding of the connecting reinforcement were identified [2]. Depending on the effective length, the position of the lattice girder truss and the roughness of the connection

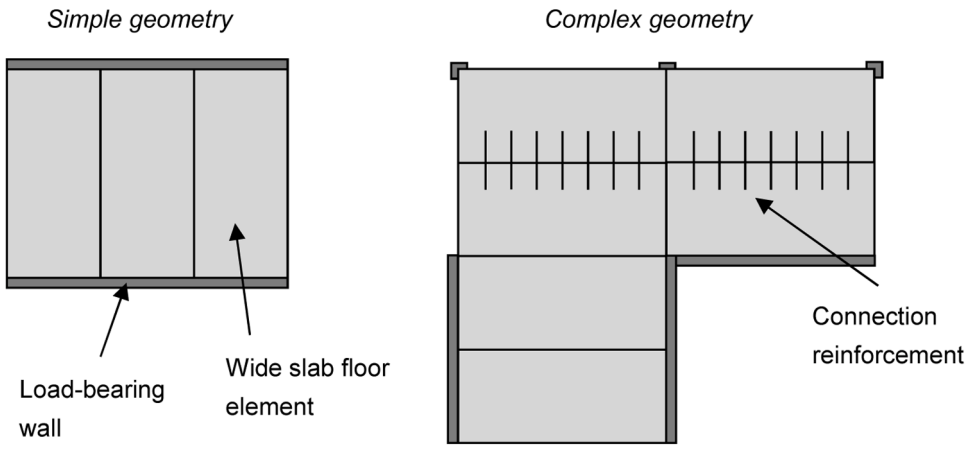

Fig. 1. Schematic top view of wide slab floor layouts: a simple geometry spanning wall-to-wall (left), and a complex geometry where connection reinforcement is required (right).

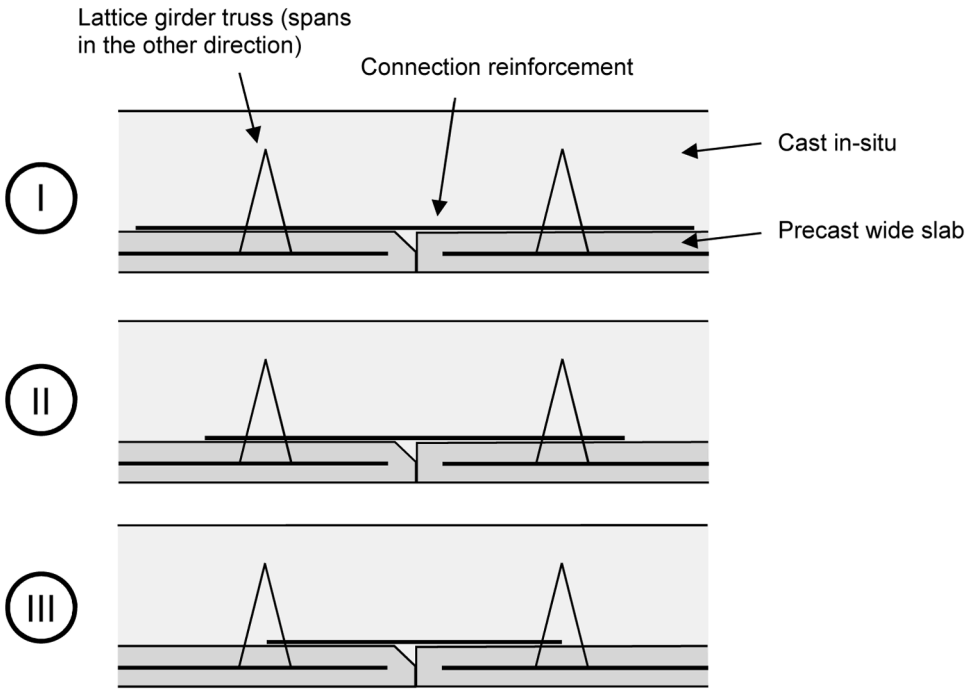

Fig. 2. Detailing methods of the joint, viewing the cross-section perpendicular to the direction of the main span (not to scale).

surface in total four failure mechanisms and their interaction have been identified. Mechanisms 1–3 act in parallel, and together they operate in series with mechanism 4 (see Fig. 3). Failure mechanism 1 is considered brittle since it relies on the tensile strength of the bond. Failure mechanisms 2–4 are considered ductile failure mechanisms – after reaching the peak strength, some deformation capacity remains. A comprehensive description of the failure mechanisms and the calculation of their capacity may be found in the main report by TNO [32].

4.3. Considered population and subpopulations

In addition to the parking garage of Eindhoven Airport, this section describes the subpopulations that have been distinguished. As discussed in Section 2.3, choosing the population or subpopulation is essential when including track record information. In identifying subpopulations, expert knowledge was included to make distinctions based on different types of floors, dimensions, reinforcement details, etc. The criteria for distinctions were based on visible properties and structural engineering knowledge as much as possible. It was tried to avoid the situation where the reliability of a structure with a known weak detail would be updated using the information of a large group of well-functioning structures where the detail is absent. The subpopulation identification was therefore performed based on the following criteria:

1. Span length, leading to typical diameters of the connection reinforcement.
2. Type of detail (as discussed in the previous section).
3. Type of concrete used: traditional or self-compacting concrete (SCC).
4. Whether mechanically roughening of the wide plate surface before in-situ casting has been performed.

If wide slabs are produced using SCC or weight-saving elements have been used, no surface treatment to promote adhesion can be performed. The roughing process is too difficult to carry out due to the consistency of the SCC or because of the weight-saving elements present on the surface of the wide slab.

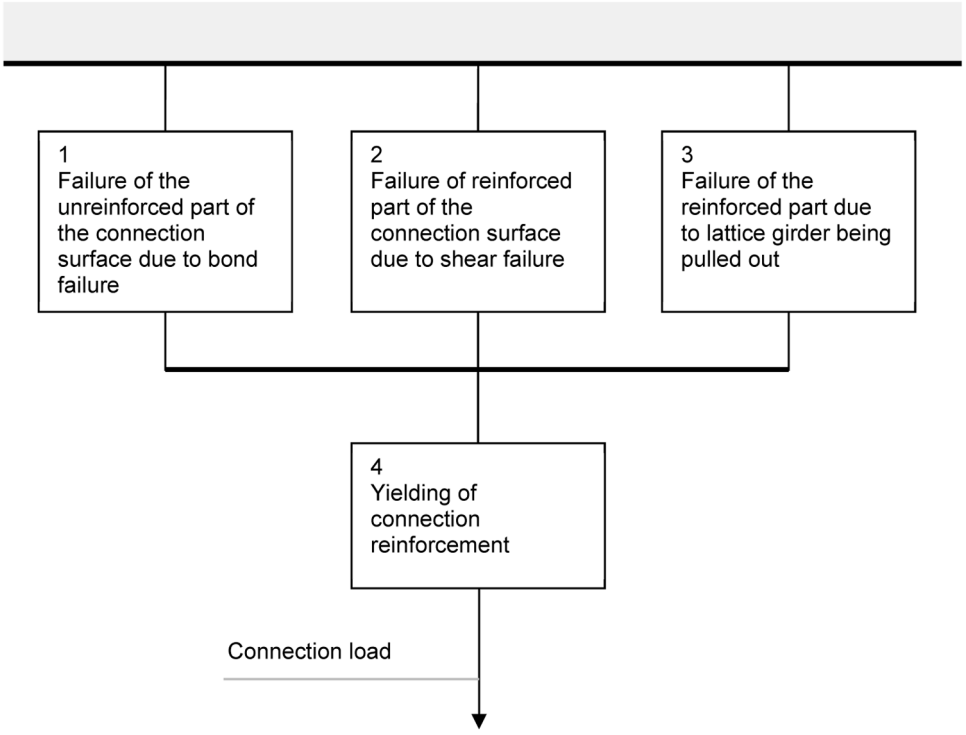

Fig. 3. Schematic representation of the combination of failure mechanisms of the joint.

The encountered variation in properties is represented by 12 subpopulations (Table 2). The subpopulations are based on common spans in buildings and their corresponding configurations. The floors were "designed" to be representative but conservative for their subpopulation. The reinforcement diameters and spacings are derived by requiring UC = 1 for the connection. In a unity check (UC), the design load effect is divided by the design strength, and the result should be smaller than or equal to unity (UC = E_d / $R_d \leq 1$). A value UC = 1 indicates that the connection strength was just sufficient according to the prevailing building regulations at the time. In the original design calculations, only failure mechanism 4 was considered; mechanisms 1–3 were not yet identified. In all considered subpopulations, the wide plates have a thickness of 70 mm. Smaller values have also been applied in practice but will result in a slightly more favourable effective height of the connection reinforcement. An edge span is considered in all configurations, as it is the least favourable in terms of occurring internal forces. A (regular) storey floor and the top floor (or roof floor) are considered for all configurations. The spacing of the connection reinforcement is adjusted to deliver a design resulting in UC = 1 for both.

4.4. Probabilistic calculation model

A calculation model has been set up to describe the resistance of each type of floor, including the critical side-to-side connection. Note that floors without this critical connection are not considered at all; they meet all requirements and should not be part of the track record. Each subpopulation is described by input parameters describing geometry (like span length and floor height, resistance properties, actions and model uncertainties). Next to mean values, also distribution types and coefficients of variation are specified in Table 3 [32]. Deterioration of the resistance was not included in the probabilistic model. If deterioration is a concern, regular it is advisable to conduct regular inspections to fulfil this assumption.

Failure of a particular floor (realisation) occurs when the overall limit state function results in a negative value: $Z < 0$. The overall limit state function is a combination of four limit state functions that are related to the four failure mechanisms of the connection (Fig. 3):

$$Z = \min\left(\max\left(Z_{e1}, Z_{p2}, Z_{p3}\right), Z_{p4}\right) \tag{7}$$

The limit state function for the elastically modelled failure

Table 2
Overview of floor and connection configurations.

Subpopulation	Span length [m]	Floor height [mm]	Conn. detail type	Connection reinforcement	Conn. length [mm]	Lattice to joint dist. [mm]	Load type	Concrete type
1	5.4	260	II	Ø8–150	476	400	Office	Trad.
2	7.2	285	I	Ø10–150	400	300	Office	SCC
3	7.2	320	I	Ø10–150	558	400	Office	Trad.
4	7.2	320	III	Ø10–150	550	550	Office	Trad.
5	7.2	320	III	Ø10–150	550	550	Office	SCC
6	7.2	320	II	Ø10–150	558	508	Office	SCC
7	7.2	320	II	Ø8–100	476	400	Office	Trad.
8	7.2	340	II	Ø10–130	400	320	Office	Trad.
9	10	360	I	Ø12–150	640	400	Office	Trad.
10	10	350	I	Ø12–150	640	370	Office	SCC
11	10	420	I	Ø16–150	803	400	Office	Trad.
12	15	450	I	Ø16–150	775	425	Parking	SCC

Table 3
Overview of random variables in the probabilistic model.

Symbol	Description	Distribution	Mean	COV
θ_R	Model uncertainty of the resistance	Lognormal	$m_{\theta R}$	$V_{\theta R}$
$m_{\theta R}$	Mean of model uncertainty of the resistance (values for prior)	Lognormal	1.0	0.3
$V_{\theta R}$	Coefficient of variation of model uncertainty of the resistance (values for prior)	Lognormal	0.2	1.0
M_{Ri}	Moment resistance of the connection for failure mechanism i, experimentally determined	[a]	[a]	[a]
M_{Rs}	Moment resistance of the support	Lognormal	[b]	0.05
μ_2	Ductility of the connection for failure mechanism 2 (shear)	Lognormal	2.15	0.51
μ_3	Ductility of the connection for failure mechanism 3 (pull out)	Lognormal	2.17	0.48
μ_4	Ductility of the connection for failure mechanism 4 (yielding)	Lognormal	3.55	0.38
θ_E	Model uncertainty of the load effect	Lognormal	1.0	0.1
G_b	Basic permanent loads following from the self-weight of the structure	Normal	[c]	0.05
G_o	Permanent loads following from sources other than self-weight	Normal	[d]	0.1
C_{0Q}	Time-invariant part of variable load following from office usage or parking	Lognormal	1.0	0.1
Q_5	Variable load following from office usage or parking, maximum in block period of 5-year	Gumbel	[e]	[e]
C_{0S}	Time-invariant part of the snow load	Lognormal	1.0	0.1
S_5	Snow load, only for roof floors exposed to the elements, maximum in block period of 5-year	Gumbel	0.365 kN/m^2	0.4
ΔT_1	Temperature difference between top and bottom of the floor due to sun radiation (uninsulated roof floors), annual maximum	Gumbel	30.0 K	0.2
ΔT_s	Equivalent temperature difference between top and bottom of the floor due to shrinkage (insulated roof floors), annual maximum	Gumbel	33.3 K	0.1

[a] The distribution type, mean and coefficient of variation follow from a calculation of the resistance in each of the four failure mechanisms using distributions for basic parameters such as concrete strength, height of the cross-section, etc.
[b] Varies depending on the floor configuration. Reinforcement diameters between 10 and 20 mm were used with spacings chosen to satisfy unity check (UC) = 1 in the original design.
[c] Varies depending on the floor height, mean values from 5.5 to 10.3 kN/m^2 are used.
[d] Varies depending on the floor type (storey or roof) and the load type, mean values from 0.5 to 2.0 kN/m^2 are used.

mechanism $i = 1$ is given by:

$$Z_{e1} = \min\left[\theta_R M_{R1} - \theta_E\left(0.07qL^2 + 0.563M_t\right), \theta_R M_{Rs} - \theta_E\left(0.125qL^2 - 1.5M_t\right)\right] \tag{8}$$

The limit state functions for plastic connection failure mechanisms $i = 2, 3, 4$ are given by:

$$Z_{pi} = \min\left[\theta_R(M_{Ri} + 0.375M_{Rs}) - \theta_E\left(0.117qL^2\right), \theta_R(M_{Ri} + 0.422{\cdot}0.75(\mu_i - 1)M_{Ri}L_\kappa/L) - \theta_E\left(0.070qL^2 + 0.563M_t\right)\right] \tag{9}$$

The meaning of the variables used in Eqs. (8) and (9) are given by:

θ_R	is the model uncertainty of the resistance;
M_{Ri}	is the moment resistance of the connection for failure mechanism i;
M_{Rs}	is the moment resistance of the support;
μ_i	is the ductility of the connection for failure mechanism i;
θ_E	is the model uncertainty of the load effect;
Q	is the distributed load caused by permanent and variable actions;
L	is the span length of the floor;
L_κ	is the distance between the point loads in the performed tests;
M_t	is the moment caused by a temperature difference or shrinkage.

The limit state function Z_{e1} follows from the linear elastic analysis of an end span. The mechanical schematisation consists of a beam that is fixed on the left ($x = 0$) and simply supported on the right ($x = L$), see Fig. 4. The two terms in Eq. (8) refer to yield in the field and yield at the clamped in support.

The limit state functions for the plastic failure mechanisms were obtained by considering a plastic deformation in the field, where the maximum rotation capacity in the joint is described by the ductility of the connection (μ_i), see Fig. 5. The ductility is defined as the ratio of the curvature at failure and the curvature at the elastic limit. The first term in Eq. (8) is the plate resistance if the ultimate deformation capacity is not an issue.

Roof floors directly exposed to the sun, such as those encountered in parking garages, suffer from temperature differences between the top and the bottom. This temperature difference, in combination with the edge constraints of the floor, results in an additional bending moment (M_t). Direct temperature load effects are virtually non-existent in most other buildings due to the applied insulation. However, these floors are sensitive to shrinkage effects due to moisture sealing. The shrinkage effects have been translated into an equivalent temperature load (also indicated as M_t). Because the impact of shrinkage reduces significantly with time as a result of concrete creep, the additional load effect is discarded after 10 years.

For regular (intermediate) floors there will be no additional moment caused by temperature differences ($M_t = 0$) and no additional load from snow. In the Eindhoven case, specific parameters were used to reflect that much more information was available for this structure due to the surveys conducted following the collapse. The impact of the information following from the structure under consideration and from other structures depends largely on the degree of correlation between the random variables in the various limit state functions. Table 4 gives an overview of the correlations used in the wide slab floor calculations.

5. Results for the case study

From the reliability analyses it followed that roof floors were most critical in terms of performance – as compared to storey floors. For brevity, in this section the results of the reliability analyses carried out for roof floors are presented. The results apply to an edge field of a floor, it is assumed that intermediate floor fields perform better. The calculations have been restricted to individual floors; system reliability has not been considered as that is no requirement according to the Dutch standards.

The update of the model uncertainty θ_R takes place under the condition that one Eindhoven top floor field fails and 8 Eindhoven storey floor fields do not fail. In addition, the survival of n buildings with 5 roof floor fields in the first 10 years of the service life (2 block durations of 5 years in the load model, see Table 2). The period of 10 years is the average age of Dutch buildings with wide slab floors. Because of the in-service proven strength, the age of the floor plays a significant role in the reliability calculation. The failure probability of a roof floor field with age t is expressed as:

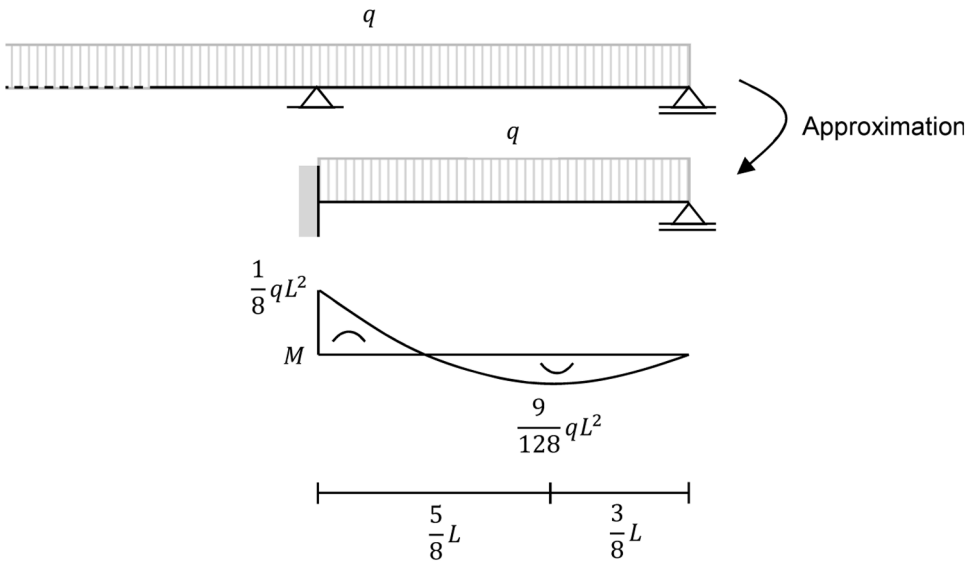

Fig. 4. Elastic analysis of a floor end field schematised as 1D beam element.

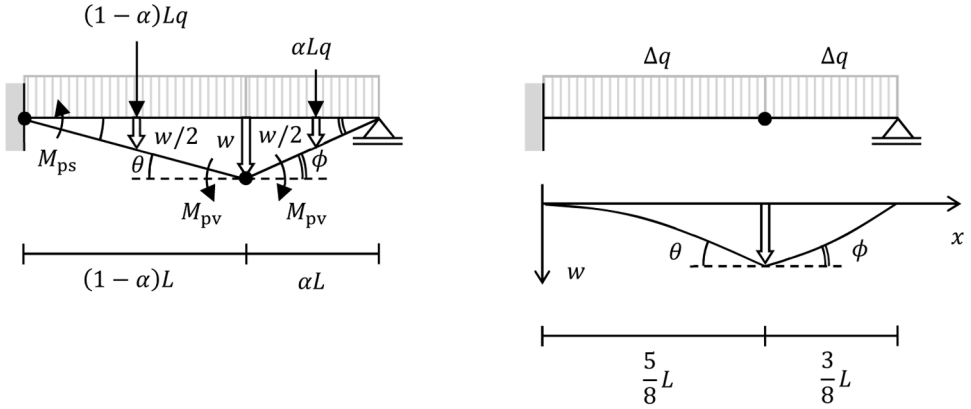

Fig. 5. Plastic analysis of the 1D beam schematisation: fully developed mechanism (left) and rotational capacity limit of the connection (right).

$$P_{f,t} = P(\text{failure of considered floor field in } t \text{ to } t+15 \text{ years} \mid \text{no failure of considered floor field in 0-}t \cap 1\times\text{failure of Eindhoven top floor field without } Q \text{ and with } \Delta T \cap 8\times\text{no failure of Eindhoven storey floor fields without } Q \cap n\times\text{no failure of building with 5 roof floor fields in 0-10 years similar to the floor under consideration}) \tag{10}$$

where Q indicates the variable load and ΔT the temperature difference between the upper and lower surface. In the above expression the $|$-sign should be read as "given" or "under the condition that" and the $\cap$-sign as "and".

The results provided in Figs. 6-8 visualise the conditional failure probability using the reliability index $\beta = -\Phi^{-1}(P_f)$. A horizontal dashed line is drawn for $\beta = 2.5$ which indicates the CC2 minimum reliability index (average Eurocode reliability class) for a reference period of 15 years in the Netherlands. The starting time for the reference periods for the structure in the three figures is chosen as 0, 5 and 10 years, respectively. This means that in Fig. 6 actually a new structure is considered and only information from other structures is available to update the reliability. In the case of zero other buildings the reliability is based solely on the prior calculation model and it is clearly not satisfying the reliability requirement. For most subpopulations (except subpopulation 11, see Fig. 6), the successful performance of 10 to 100 other buildings may lead to the qualification of being just sufficient. In Figs. 6-8 also the behaviour of the structure under consideration itself is taken into account. The inclusion of this data helps to increase the reliability estimates. Note that a maximum reliability index of $\beta = 5$ is used in the plots because higher values could not be accurately calculated in the Monte Carlo simulation (and provide no added value).

Subpopulations 1–11 are insulated roof floors subject to shrinkage. The shrinkage gradient occurs only in the first years of life span and has largely disappeared after about 10 years. The reliability in the period

Table 4
Overview of correlations in time and between floors.

Symbol	Definition	In time (one floor)	Between floors, same building	Between floors, other building
G_{DL}	Dead load	1	0.8	0
G_{SDL}	Super-imposed dead load	1	0.8	0
C_{0Q}	Time-independent component of imposed load	1	1	0
Q	Imposed load	0	0.7	0
C_{0S}	Time-independent component of snow load	1	1	0
S	Snow load	0	0.7	0
ΔT	Temperature difference	0	0.7	0
ΔT_s	Equivalent temperature difference for shrinkage	1	0.7	0
M_R	Moment resistance	1	0	0
θ_E	Model uncertainty load effect	1	1	0
θ_R	Model uncertainty moment resistance	1	0.8	0
$m_{\theta R}$	Mean of θ_R	1	1	1
$V_{\theta R}$	Coefficient of variation of θ_R	1	1	1

0–10 years is low due to the presence of the large load following from shrinkage in the first 10 years. (The snow load is not included in the first 10 years of analysis, because meteorological data in the Netherlands show that in the past 10 years snow loads were much lower than would follow from the statistical model.) After 10 years the shrinkage does not play a role anymore. This explains the large increase of reliability for subpopulations 1–11 in the period 10–25 years (Fig. 8).

Subpopulation 12 is a roof floor directly subject to solar radiation, similar to the collapsed Eindhoven parking garage. In the probabilistic analysis, the limit state is calculated using the maximum load including the temperature difference or including the snow load, but not together. It is observed that even roof floors with an age of 10 years do not show sufficient reliability. This is due to the significant influence of the temperature load, which is constantly present during the life of the structure.

Given the results, only the roof floors of subpopulations 1–11 may provide sufficient reliability given that quite a large number of buildings (n) can be identified in the population with a similar floor type. Given that the building, of which the floor under consideration is part, has survived for at least 5 years, fewer buildings with good performance are needed to arrive at a sufficient reliability level. According to the calculations subpopulation 12 will never possess sufficient reliability.

6. Discussion

The results presented in the previous section indicate the effect of the track record in terms of the updated reliability indices. The increase in reliability with the number of buildings n is attributed to the update of the model uncertainty for the resistance (θ_R). The update is performed within the application of the Bayesian Monte Carlo (BMC) method (Section 3.3). It is interesting to have a look at the effect of the track record on the distribution the posterior predictive distribution of θ_R:

$$f_{\theta R}^{(p)}(\theta_R) = \int_0^\infty \int_0^\infty f_{\theta R}(\theta_R|m_{\theta R}, V_{\theta R}) f_{m_{\theta R}, V_{\theta R}}(m_{\theta R}, V_{\theta R}|D)\mathrm{d}m_{\theta R}\mathrm{d}V_{\theta R} \approx \frac{1}{m}\sum_{i=1}^{m} f_{\theta R}(\theta_R|m_{\theta R,i}, V_{\theta R,i}) \quad (11)$$

where $f_{\theta R}$ is the lognormal distribution of θ_R, here parametrised through mean value $m_{\theta R}$ and coefficient of variation $V_{\theta R}$. The bivariate posterior distribution is denoted by $f_{m\theta R, V\theta R}$ and is conditional upon the data D in the track record. The integral may be approximated using the m posterior samples obtained via the BMC method.

Subpopulation 6 was selected to display the posterior predictive distribution because it represents a commonly found wide slab floor configuration. The scatter plots of the posterior samples and the corresponding posterior predictive functions are provided in Fig. 9. It is seen that as the number of buildings n increases, the mean value of θ_R becomes larger (positive bias) and the dispersion decreases. As an alternative to the adopted procedure, in which the m posterior samples from the BMC method are used directly, a continuous distribution could have fitted to the posterior predictive distribution. Although this would have given more insight, the resulting distribution is not lognormal, nor does it follow another elementary distribution. Hence, producing a fit would have resulted in the introduction of an unnecessary error. In the scatter plots, only a limited number of points are shown for clarity – more were used in the reliability calculations.

The target number of samples for the posterior was 10^4. Only for

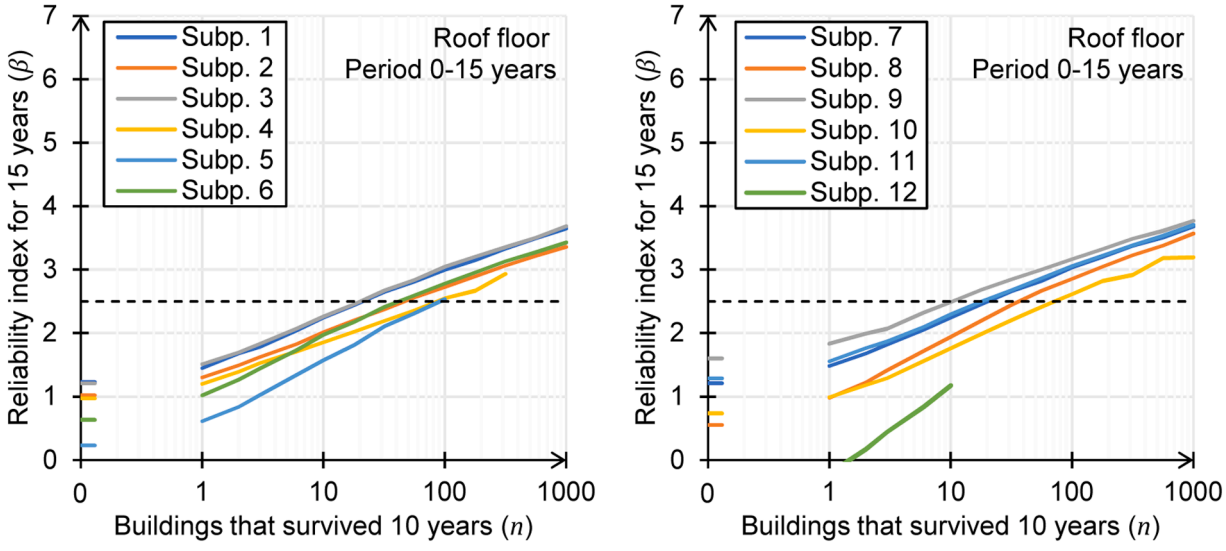

Fig. 6. Reliability index in period 0–15 years versus the number of similar buildings that have survived for 10 years.

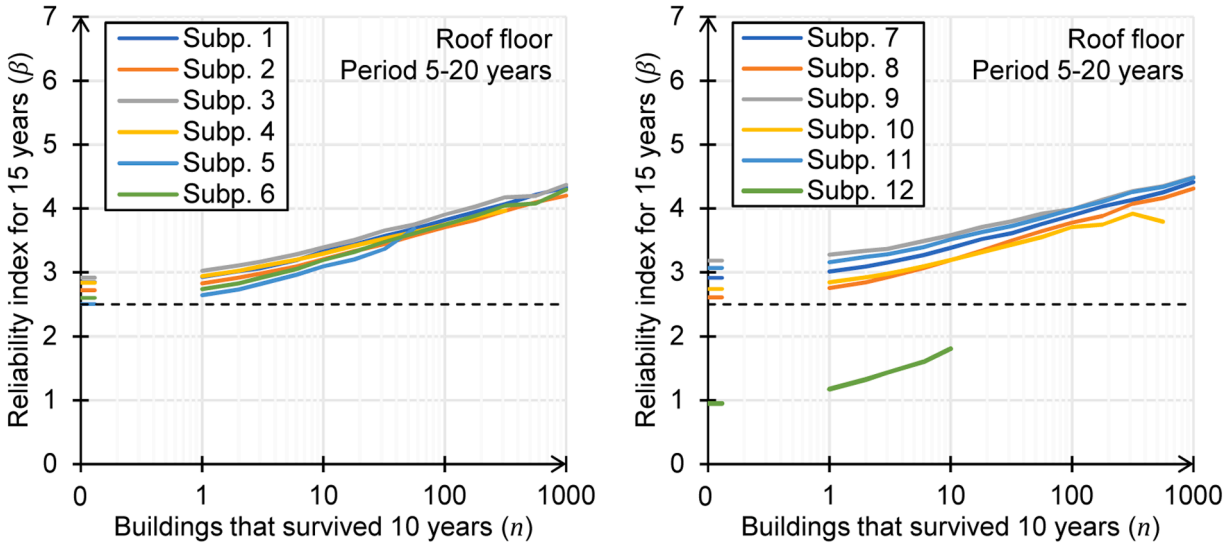

Fig. 7. Reliability index in period 5–20 years versus the number of similar buildings that have survived for 10 years.

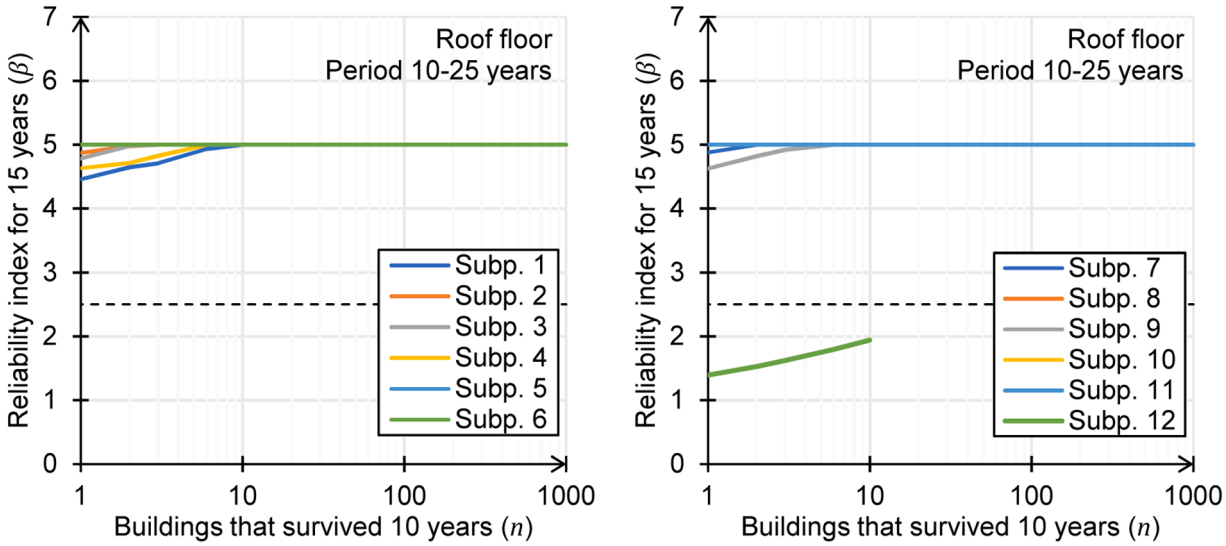

Fig. 8. Reliability index in period 10–25 years versus the number of similar buildings that have survived for 10 years.

large values of n (562 and 1000) the target was reduced to $2{\cdot}10^3$ samples to reduce the computational effort. The target was determined experimentally, witnessing no significant change in calculated reliability values when increased further. The evaluation of the likelihood given a random prior sample, was repeated until the target number of samples for the posterior was reached. This procedure required about 10^5 prior samples with an acceptance ratio of about 10 % for small n, up to about $2{\cdot}10^6$ prior samples with an acceptance ratio of 0.1 % for large n. In the subsequent reliability analysis, $5{\cdot}10^3$ realisations of θ_R were produced for each posterior sample, resulting in a total of 10^7 to $5{\cdot}10^7$ samples. In cases where the reliability of the subpopulation is very low, the acceptance ratio becomes extremely small for large n. In these cases no reliability calculation could be performed (Figs. 6-8, subpopulation 12 with $n > 10$). The computation time for each subpopulation on a standard office laptop was about 10 minutes. If the evaluation of the limit state function would require significant computational effort, then the total calculation time for determining the posterior distribution using a Monte Carlo-based algorithm would significantly increase.

Sensitivity analyses were performed concerning the magnitude of imposed loads, the connection ductility, the diameter of the lattice girder reinforcement, possible settlements, the post-processing of wide slabs, a rotational spring instead of clamped support, a statically determined floor field, the occurrence of two critical joints instead of one, and the hypothetical collapse of two Eindhoven parking garages. Only small changes in the resulting reliability indices occurred in the sensitivity analyses – with two notable exceptions. The magnitude of the imposed load made a significant difference. When the mean value of the imposed load is lowered, higher reliability indices are obtained for all subpopulations. However, its reliability is lower when a building has been vacant for a long time. In the latter case, no in-service strength is proven during the vacant period. Combined with detailing type III, the post-processing (roughening) of wide slabs also significantly improved the reliability. In this detailing type, the connection strength is governed by the concrete bond strength, which is reduced significantly without post-processing of the wide slab floor elements.

In several buildings, proof load tests were performed. The magnitude of the proof load, when expressed as a fraction of the characteristic imposed load ($Q_p = \xi\, Q_k$), ranged from $\xi = 0.67$ to 1.26. The target load level was incorporated into the track record to study its effect on reliability. With the highest target load ($\xi = 1.26$), the reliability of the

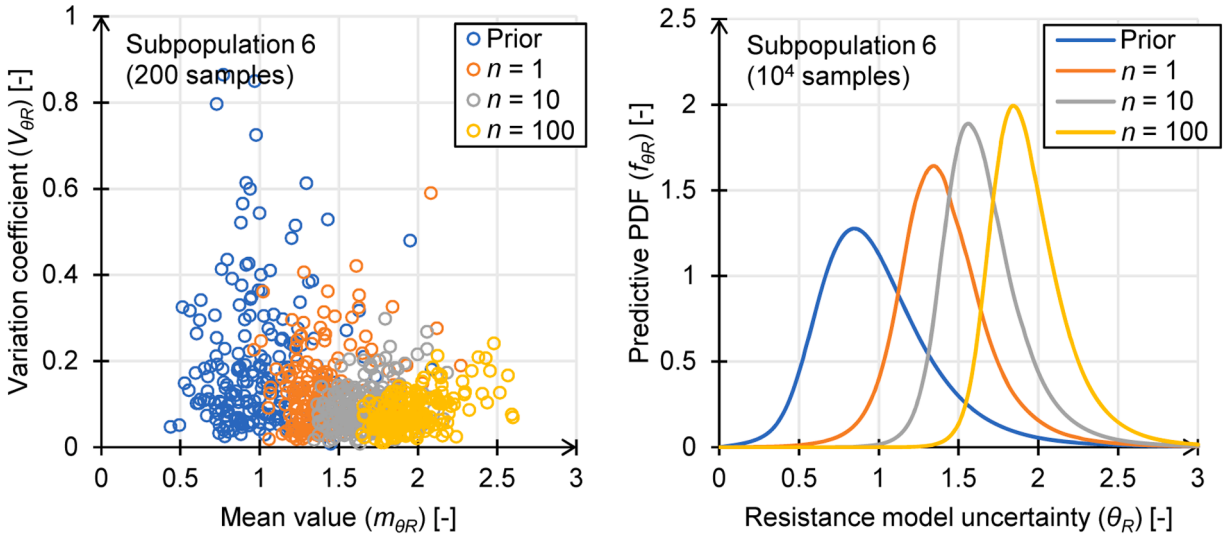

Fig. 9. Effect of the track record on the posterior distribution: scatter plots of a limited number of samples (left) and the corresponding approximative posterior predictive probability density functions (right).

tested floor itself improved markedly, but the other floors in the sub-population benefitted only very little.

7. Conclusions

The current article provides a step forward in the probabilistic assessment of existing structures by accounting for the track record. The track record comprises the performance of the object itself, up to the time of assessment, and the performance of similar objects, including their (loading) conditions. The latter is referred to as the 'mega-experiment' and allows for an update of the resistance model uncertainty (θ_R). Use is made of statistical inference via the application of the Bayesian method to perform the update of structural reliability.

Because of the believed poor engineering of the highly loaded longitudinal joints and the anticipated variations among the different applied configurations, a low informative prior was adopted. The prior's average was based on a set of laboratory tests carried out as part of the investigation following the roof failure of the parking garage of Eindhoven. In the Bayesian updating process each possible sub-population (12 in total) was updated on the basis of the corresponding track record. The track record consisted of the behaviour of the structure itself up to the time of assessment, as well as the survival of a certain number of buildings with floors having a similar configuration and detailing. Each track record included the failed floor of Eindhoven Airport to err on the conservative side.

The adopted procedure allowed rational judgments about the conditions under which the floors can be considered sufficiently reliable and under which the Dutch reliability requirement is not met. The insulated roof floors appeared to be the most critical due to the shrinkage load in the first 10 years after construction. This result was attributed to the low strength and deformation capacity of the critical joint. In addition, roof floors irradiated directly by sunlight did not perform well.

Fortunately, this study identified numerous subpopulations with sufficient reliability. The outcomes of the study enabled a significant acceleration in the assessment process by indicating which floor configurations do not need further investigation. This outcome underlines the practical value of the procedure. Finally, it is important to note that in most cases, neither a classical procedure (lab tests and standard analysis) nor solely relying on the track record was sufficient to reach this conclusion.

CRediT authorship contribution statement

R. de Vries: Writing – original draft. **R.D.J.M. Steenbergen:** Writing – original draft. **A.C.W.M. Vrouwenvelder:** Writing – review & editing.

Declaration of competing interest

The authors declare that they have no known competing financial interests or personal relationships that could have appeared to influence the work reported in this paper.

Appendix A: Monte Carlo updating algorithm

In the Monte Carlo simulation used to update the structural reliability, two steps are performed. In the first step, the posterior distribution is calculated using the algorithm schematically presented in Fig. A.1. The uncorrelated prior distributions for mean and variation coefficient of the model uncertainty θ_R are converted to possibly correlated pairs ($m_{\theta R}$, $V_{\theta R}$) that describe the posterior distribution by the Bayesian Monte Carlo (BMC) method. The algorithm is run until enough samples of the posterior have been collected. In the second step, the updated posterior distribution is used to perform the reliability update. The Monte Carlo algorithm to perform this integration of the posterior is presented in Fig. A.2. In essence, for each posterior sample a regular reliability analysis is performed. An important difference with the first step (Fig. A.1) is the consideration of just a single component – hence only correlations in time (autocorrelation) need to be considered.

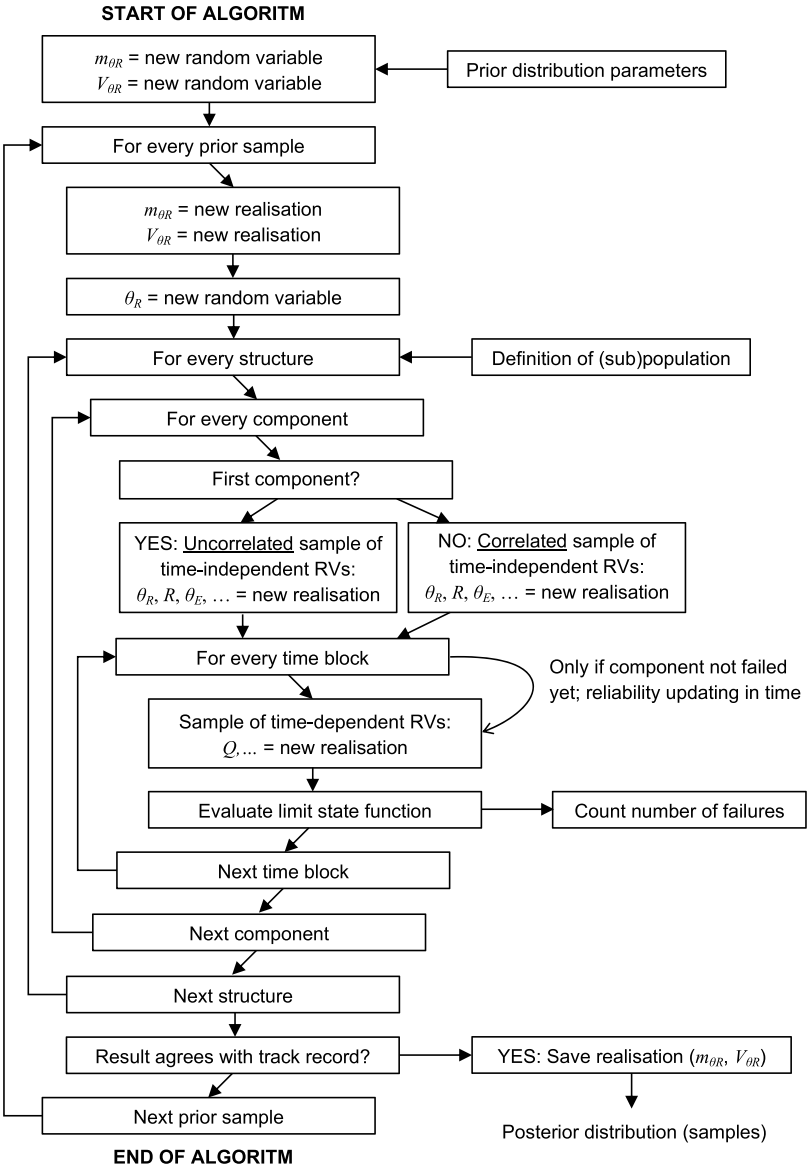

Fig. A.1. Schematisation of the BMC method to calculate the posterior.

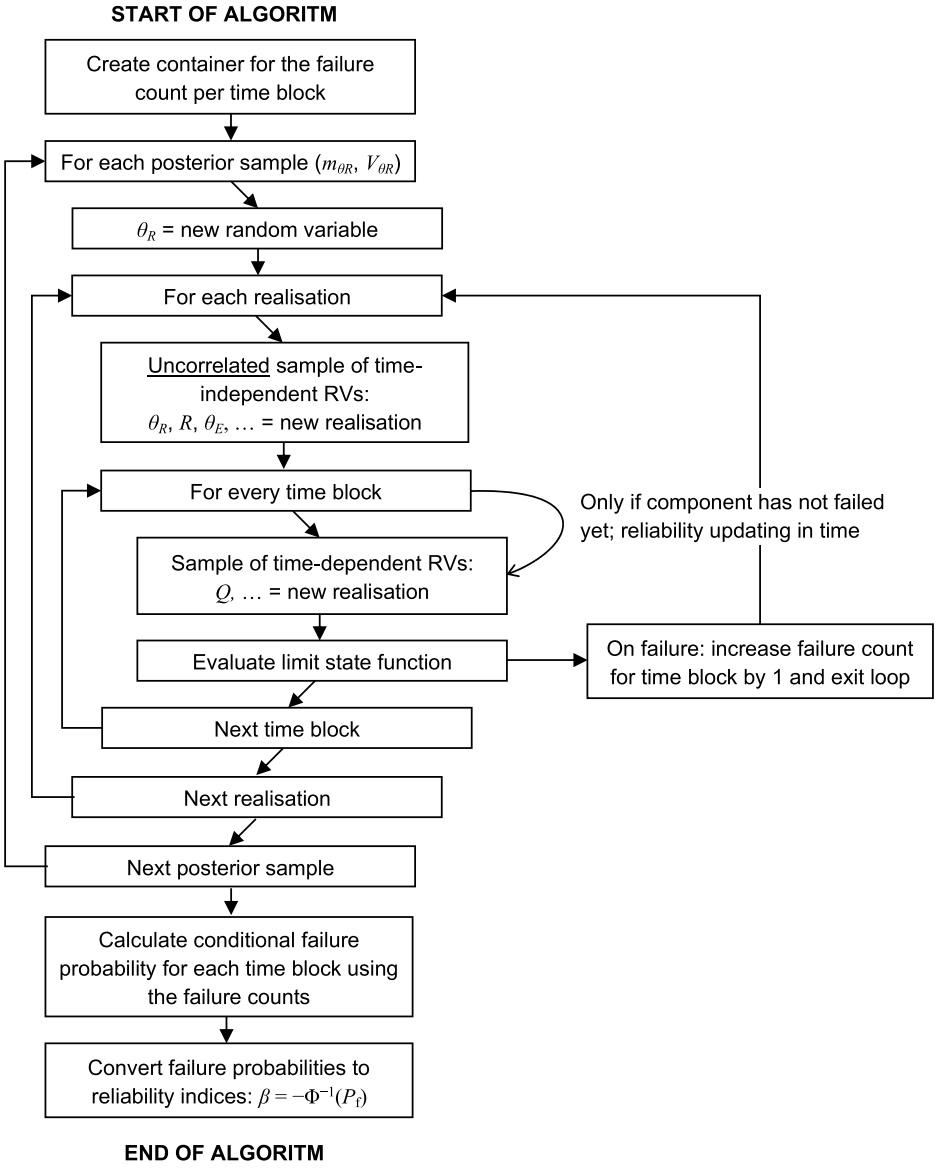

Fig. A.2. Schematisation of the reliability calculation with posterior.

References

[1] TNO, Onderzoek naar de technische oorzaak van de gedeeltelijke instorting van de in aanbouw zijnde parkeergarage P1 Eindhoven Airport. TNO-2017-R11127. 2017.
[2] Hageman, A., Onderzoek constructieve veiligheid breedplaatvloeren in bestaande utiliteitsgebouwen – Voorstellen voor en achtergronden bij rekenregels voor beoordeling van bestaande bouw. 9780-1-0. 2019.
[3] CEN, Eurocode 0: basis of structural design. Standard, EN 1990+A1+A1/C2:2019 2019.
[4] ISO. ISO 2394:2015 general principles on reliability for structures. International Organization for Standardization; 2015.
[5] Ditlevsen O, Madsen HO. Structural reliability methods. book. John Wiley & Sons; 1996.
[6] Jeffreys H. Theory of probability. 3rd ed. Book: Oxford University Press; 1961.
[7] Robert CP, Chopin N, Rousseau J. Harold Jeffreys's theory of probability revisited. Stat Sci 2009;24(2):141–72.
[8] Lindley DV. Introduction to probability and statistics from a bayesian viewpoint - Part 2: inference. Book: Cambridge University Press; 1965.
[9] Box G, Tiao GC. Bayesian inference in statistical analysis. Book, Addison-Wesley; 1973.
[10] Benjamin, J.R. and C.A. Cornell, Probability, statistics, and decision for civil engineers. Book, McGraw-Hill 1970.
[11] Peterka V. Bayesian system identification. Automatica 1981;17(1):41–53.
[12] Madsen HO, Krenk S, Lind NC. Methods of structural safety. Englewood Cliffs, New Jersey: Prentice Hall; 1986. p. 403.
[13] Diamantidis D. Reliability assessment of existing structures. Eng Struct 1987;9(3):177–82.
[14] Natke HG. Updating computational models in the frequency domain based on measured data: a survey. Probabilistic Eng Mech 1988;3(1):28–35.
[15] Jiao G, Moan T. Methods of reliability model updating through additional events. Struct Saf 1990;9(2):139–53.
[16] Straub D, Papaioannou I. Bayesian updating with structural reliability methods. Eng Mech 2015;141(3).
[17] Engelund S, Rackwitz R. On predictive distribution functions for the three asymptotic extreme value distributions. Struct Saf 1992;11.
[18] Ditlevsen O, Vrouwenvelder A. Objective" low informative priors for Bayesian inference from totally censored Gaussian data. Struct Saf 1994;16:175–88.
[19] Raiffa H, Schlaifer R. Applied statistical decision theory. Book, Harvard University, Division of Research, Graduate School of Business Administration; 1961.
[20] Hornberger GM, Spear RC. Eutrophication in peel inlet—I. The problem-defining behavior and a mathematical model for the phosphorus scenario. Water Res 1980;14(1):29–42.
[21] Dilks DW, Canale RP, Meier PG. Development of Bayesian Monte Carlo techniques for water quality model uncertainty. Ecol Modell 1992;62(1):149–62.
[22] Metropolis N, et al. Equations of state calculations by fast computing machines. Chem Phys 1953;21(6):1087–91.
[23] Hastings WK. Monte Carlo sampling methods using Markov Chains and their applications. Biometrika 1970;57(1):97–109.

[24] Geman S, Geman D. Stochastic relaxation, Gibbs distributions, and the Bayesian restoration of images. IEEE Trans Pattern Anal Mach Intell 1984;6(6).
[25] Qian SS, Stow CA, Borsuk ME. On monte carlo methods for bayesian inference. Ecol Modell 2003;159:269–77.
[26] Kloek T, Van Dijk HK. Bayesian estimates of equation system parameters: an application of integration by Monte Carlo. Econometrica 1978;46(1):1–19.
[27] Press WH, Farrar GR. Recursive stratified sampling for multidimensional monte carlo integration. Comput Phys 1990;4(2):190–5.
[28] Stroustrup B. The C++ programming language. 4th edition. Book, Pearson Education; 2013.
[29] Madsen HO. Model updating in reliability theory. In: Proceedings of the 5th International Conference on Application of Statistics and Probability in Civil Engineering (ICASP); 1987. p. 564–77.
[30] NEN. NVN 6725:2008 vrijdragende systeemvloeren van vooraf vervaardigd beton. Nederlands Normalisatie-instituut; 2008.
[31] NEN. NEN-EN 13747:2005+A2:2010 vooraf vervaardigde betonproducten - Breedplaatvloeren. Nederlands Normalisatie-instituut; 2010.
[32] TNO, Probabilistische kwantificering van de veiligheid van bestaande breedplaatvloeren. TNO-2022-R10122. 2022.